Editors' Suggestion

Optical Kinetic Theory of Nonlinear Multimode Photonic Networks

Arkady Kurnosov,[1] Lucas J. Fernández-Alcázar,[2,3] Alba Ramos,[2,3] Boris Shapiro,[4] and Tsampikos Kottos[1]
[1]Department of Physics, Wave Transport in Complex Systems Laboratory, Wesleyan University, Middletown, Connecticut 06459, USA
[2]Institute for Modeling and Innovative Technology, IMIT (CONICET - UNNE), Corrientes W3404AAS, Argentina
[3]Physics Department, Natural and Exact Science Faculty, Northeastern University of Argentina, Corrientes W3404AAS, Argentina
[4]Technion - Israel Institute of Technology, Technion City, Haifa 3200, Israel

(Received 23 October 2023; accepted 4 April 2024; published 8 May 2024)

Recent experimental developments in multimode nonlinear photonic circuits (MMNPCs), have motivated the development of an optical thermodynamic theory that describes the equilibrium properties of an initial beam excitation. However, a nonequilibrium transport theory for these systems, when they are in contact with thermal reservoirs, is still *terra incognita*. Here, by combining Landauer and kinematics formalisms we develop a universal one-parameter scaling theory that describes the whole transport behavior from the ballistic to the diffusive regime, including both positive and negative optical temperature scenarios. We also derive a photonic version of the Wiedemann-Franz law that connects the thermal and power conductivities. Our work paves the way toward a fundamental understanding of the transport properties of MMNPCs and may be useful for the design of all-optical cooling protocols.

DOI: 10.1103/PhysRevLett.132.193802

Introduction.—Recently, we have witnessed a surge in understanding and harnessing the convoluted behavior of light propagation in multimode nonlinear photonic circuits (MMNPCs). These platforms have been used for exploring exotic optical phase transitions [1–4], beam self-cleaning phenomena [5–7], spatiotemporal mode locking [8], multimode solitons [9], etc. In parallel, their implementation in fiber-optical communications might resolve urgent technological needs associated with the looming information "capacity crunch" [10,11] or the quest for high-power light sources [8].

Nonlinearities lead to multiwave mixing processes or photon-photon "collisions" through which the many modes can exchange energy via a multitude of possible pathways. Evidently, modeling, predicting, and harnessing the response of such exceedingly complex configurations is practically impossible using conventional brute-force time-consuming computations that obscure the underlying physical laws. Fortunately, a new universal approach inspired by concepts from statistical thermodynamics emerged recently [12]. Under thermal *equilibrium* conditions, the methodology has identified intrinsic variables (optical temperature T and chemical potential μ) that play the role of optical thermodynamic forces leading an initial beam excitation to a Rayleigh-Jeans (RJ) thermal state [4,12,13] —a key tenet of this theory that has been confirmed using multimode optical fibers and time-synthetic photonic lattices [14–17].

Here, we develop a universal transport theory that describes the *nonequilibrium* steady states generated in a MMNPC (a photonic junction) when it is in contact with two optical reservoirs at different optical temperatures and/or chemical potentials. The proposed optical kinetics framework allows for the evaluation of various kinetic coefficients like optical power and thermal conductivities in full analogy with physical kinetics in condensed matter [18]. The presence of two conserved quantities (total optical power and electrodynamic momentum flow, referred to below as internal energy) requires considering the coupling between thermal and power currents mediated by nonlinear interactions—a complication that is not present in phonon heat transport in solids. Using a combination of Landauer (ballistic limit) and Boltzmann (diffusive limit) transport theories, we established a one-parameter scaling theory that describes the crossover from a ballistic to a diffusive limit as the size of the photonic junction increases beyond a characteristic thermalization length scale l_T. Our universal theory is applicable for both positive and negative optical temperatures and incorporates the specific characteristics of the topology of the reservoirs and their contacts with the optical junction. Furthermore, the dependence of the transport features in various physical parameters (e.g., optical temperature, chemical potential, nonlinearity strength, system size, etc.) is encoded *only* in the ratio of the thermalization length l_T over the system size. Finally, we analyze the interdependence of optical power and heat transport by deriving the photonic analog of Wiedemann-Franz law that connects the thermal and power conductances. Their ratio is inversely proportional to temperature—as opposed to the linear temperature behavior for typical thermoelectric devices—which is a signature of relaxation scale separation between the energy and power currents. The optical kinetic theory approach that has been developed in this work is general. It sets the basis

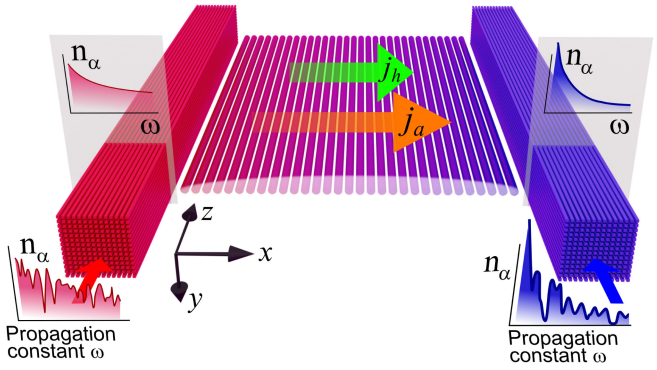

FIG. 1. The two photonic reservoirs (L/R) consist of a large number of coupled nonlinear waveguides. We initially inject two beams at each of the reservoirs with different internal energy and power. At the steady state, the power distribution is given by a RJ thermal state with predetermined temperatures $T_{L/R}$ and chemical potentials $\mu_{L/R}$. After reaching a thermal state, the two reservoirs are coupled by an optical junction that transports heat and power currents. For intermediate, but large, length scales these currents acquire a quasi-steady-state j_h, j_a.

for the development of novel thermophotonic devices and paves the way for the design of novel photonic refrigerators or engines.

Physical setting.—For presentation purposes, we consider the specific setup shown in Fig. 1. It consists of two optical reservoirs and a junction that facilitates thermal and power transport between the reservoirs. The left (L) and right (R) reservoirs consist of arrays of (weakly) nonlinear coupled optical waveguides (or, alternatively, multimode or multicore optical fibers) supporting a finite (but large) number $\gamma = 1, \ldots, M$ of linear supermodes $|\phi_\gamma^{(L/R)}\rangle$—all propagating along the paraxial direction z with propagation constants $\omega_\gamma^{(L/R)}$. At each reservoir, we launch a beam prepared at some state $|\Psi^{(L/R)}(z=0)\rangle = \sum_\gamma C_\gamma^{(L/R)} |\phi_\gamma^{(L/R)}\rangle$, where $C_\gamma^{(L/R)} = \langle \phi_\gamma | \Psi^{(L/R)} \rangle$ are the projection coefficients to their supermodes. Initially, the reservoirs are decoupled from one another and, therefore, their total optical power $\mathcal{N}^{L/R}(\{C_\gamma^{(L/R)}\}) = \sum_\gamma |C_\gamma^{(L/R)}|^2 \equiv A^{(L/R)}$ and internal energy $\mathcal{H}^{L/R}(\{C_\gamma^{(L/R)}\}) \approx \sum_\gamma |C_\gamma^{(L/R)}|^2 \omega_\gamma \equiv E^{L/R}$ are constants of motion that are used to determine the optical temperature T and chemical potential μ that define their RJ thermal state $n_{L/R}(\omega_\gamma^{(L/R)}) = \langle |C_\gamma^{(L/R)}|^2 \rangle \equiv [T_{L/R}/(\omega_\gamma - \mu_{L/R})]$ [4,12,19,20].

Once each reservoir reaches a thermal equilibrium with $(T_L, \mu_L) \neq (T_R, \mu_R)$ at paraxial distances z_R, they are coupled with an optical junction: an array of coupled (weakly) nonlinear single-mode waveguides supporting $\alpha = 1, \ldots, N$ linear supermodes $|\phi_\alpha^{(J)}\rangle$ that propagate with paraxial propagation constants $\omega_\alpha^{(J)}$.

The junction facilitates heat and power transport between the reservoirs. Obviously, the characteristics of the junction, i.e., coupling between waveguides, nonlinearity strength, size, etc., will determine these currents, and, in turn, the paraxial length z_{GT} at which the whole system reaches a global thermalization. We are not interested in the behavior of the system at these (practically irrelevant) large paraxial length scales. Rather, we focus our investigation on a physically relevant intermediate (but still large) length scale $z_{\mathrm{tr}}(\sim 10^{-2} z_R) < z \ll z_{\mathrm{GT}}(\sim 50 z_R)$, where (after a transient paraxial length z_{tr}) the currents through the junction acquire (quasi-)steady-state values [21]. For physical implementations, see Supplemental Material [21] and Refs. [14,15,17]. We develop a nonequilibrium transport theory for power and heat transfer at these intermediate length scales.

Mathematical modeling.—The beam dynamics at the junction and the left and right reservoirs are described by a temporal coupled mode theory (TCMT),

$$i\frac{d\Psi_l}{dz} = -\sum_j J_{lj}\Psi_j + \chi|\Psi_l|^2\Psi_l, \tag{1}$$

where $\Psi_l \equiv \langle l|\Psi\rangle$ is the field amplitude at the lth waveguide, $\epsilon_l = -J_{ll}$ is its propagation constant, and χ is the Kerr nonlinearity coefficient. The connectivity of the network is dictated by the coupling coefficients $J_{lj} = J_{jl}^*$. At the junction $J_{lj} = J\delta_{l,l\pm1}$ ($\epsilon_l = \epsilon = 0$). The corresponding linear dispersion relation takes the form $\omega_\alpha^{(J)} = -2J\cos(k)$ where the wave vector $k \in [-\pi, \pi]$. The two reservoirs consist of a square lattice of $N_r = 40 \times 40 = 1600$ waveguides with $J_{lj} = J$. To avoid spectral degeneracies, we consider propagation constants given by a uniform distribution $\epsilon_l \in [-(W/2), (W/2)]$ with $W = 0.5$. The junction-reservoir coupling is $J_{b-r} = 0.2J$. We have confirmed via direct dynamical simulations of the composite system the existence of a (quasi-)steady-state regime, maintained for propagation distances z_{GT}, during which the temperature and chemical potential at each reservoir remain (approximately) constant when $M \gg N$. We have further validated our theory using Monte Carlo reservoirs, which are ignorant of their specific topology [22].

Onsager matrix formalism.—We consider the power $a(x)$ and energy $h(x)$ densities at any junction segment $(x, x+dx)$ which includes many unit cells. At the (quasi) stationary regime, these segments are at local equilibrium characterized by a local temperature and chemical potential, i.e., $T = T(x)$, $\mu = \mu(x)$ which slowly change with the position. The currents are evaluated by expanding the spatial gradients of μ, T up to the first term [23,24],

$$\mathbf{j} = \hat{\mathcal{L}}\mathbf{f}, \qquad \hat{\mathcal{L}} = \begin{pmatrix} \mathcal{L}_{aa} & \mathcal{L}_{aq} \\ \mathcal{L}_{qa} & \mathcal{L}_{qq} \end{pmatrix}. \tag{2}$$

Above, $\mathbf{j} = (j_a, j_q)^T$, where $j_a, j_h, j_q = j_h - \mu j_a$ are the power, energy, and heat currents, and $\hat{\mathcal{L}}$ is the Onsager

matrix, while the affinities $\mathbf{f} = (-\nabla\mu/T, \nabla(1/T))^T$ are the thermodynamical forces that induce the currents. For systems preserving time reversal symmetry, the Onsager reciprocity relations hold, i.e., $\mathcal{L}_{qa} = \mathcal{L}_{aq}$ [23,31].

We distinguish between two limiting cases of short $N \ll l_T$ (ballistic) and long $N \gg l_T$ (diffusive) junctions where $l_T = v_g z_T$, v_g is a typical group velocity of the linear supermodes, while $z_T = z_T(\chi, J, T, a)$ is a relaxation distance that dictates the thermalization process of a nonequilibrium state in the isolated junction toward its RJ distribution [20,25]. Strictly speaking, the concept of local equilibrium used in Eqs. (2) applies to the diffusive regime only while in the ballistic regime; the meaningful quantities are the temperatures $T_{L,R}$ and chemical potentials $\mu_{L,R}$ of the two reservoirs. In this case, we can formally define $\nabla T \equiv (T_R - T_L)/N$; $\nabla\mu \equiv (\mu_R - \mu_L)/N$ to have unified notations for both regimes.

The various transport coefficients are extracted from the Onsager matrix elements (2). For example, the power conductivity is $\sigma \equiv \mathcal{L}_{a,a}/T$, the thermal conductivity is $\varkappa = \det\hat{\mathcal{L}}/(T^2\mathcal{L}_{aa})$, while the Seebeck and Peltier coefficients that describe thermopower transport are $S = \mathcal{L}_{aq}/(T\mathcal{L}_{aa})$ and $\Pi = T\,S$ (see Supplemental Material for details [21]).

Ballistic regime: In this regime, the nonlinear interactions are not able to enforce mixing among the linear modes. The power and energy fluxes through the junction are evaluated using Landauer's theory [26]

$$j_{a(h)} = \int d\omega\, t(\omega)\omega^s [n_L(\omega) - n_R(\omega)], \tag{3}$$

where $s = 0$ ($s = 1$) for power (energy) current. We further assume that the transmittance $t(\omega) = t_0 = \text{const}$ for all supermodes in the band $[-2J, 2J]$ and zero otherwise. Equation (3) can be evaluated analytically, thus allowing us to extract the Onsager matrix elements (see Supplemental Material [21])

$$\mathcal{L}_{aa} = t_0 N \frac{4JT^2}{\mu^2 - 4J^2}; \qquad \mathcal{L}_{qq} = t_0 N 4JT^2$$
$$\mathcal{L}_{aq} = \mathcal{L}_{qa} = -t_0 N T^2 \ln\left(1 - \frac{4J}{-\mu + 2J}\right), \tag{4}$$

where $T = (T_L + T_R)/2$, $\mu = (\mu_L + \mu_R)/2$, and $|\Delta\mu| \ll |\mu| - 2J$ and $\Delta T \ll T$ (linear response regime). Equations (4) allow us to derive exact expressions for the transport coefficients $\sigma, \varkappa \propto N$. We conclude that when $l_T \gg N$, Fourier's law is violated.

While the weak nonlinear interactions cannot enforce sufficient mode-mode mixing, they can induce a nonlinear frequency shift $\omega_\alpha^{(J)} \to \omega_\alpha^{(J)} + 2a\chi$ (see Supplemental Material [21] and Ref. [27]) which might affect the currents. Nevertheless, Eq. (3) still applies with the modification that the transmittance is constant t_0 inside a *shifted* frequency window $\omega^{(J)} \in [-2J + 2\chi a, 2J + 2\chi a]$ and zero everywhere else. As a result, Eq. (4) still applies with the substitution $\mu_{L,R} \to \mu_{L,R} - 2a\chi$. This correction $j_{a(h)} \to j_{a(h)}^{(\chi)}$ is insignificant for high temperatures, $T \sim |\mu| \gg 2a\chi$ but it becomes important when $|\mu| \sim 2J$.

Diffusive transport: In the other limiting case of $N \gg l_T$, the nonlinear mode-mode interactions become a dominating mechanism of power and heat transport. They are responsible for a local equilibrium within l_T segments of the junction, thus allowing us to define slowly varying local temperatures $T(x)$ and chemical potentials $\mu(x)$. In parallel, the modal occupations become a local quantity, i.e., a function of coordinate x, wave vector k, and propagation distance z, $n = n(x, k, z)$. We proceed by invoking a kinetic equation (KE) approach [27]

$$\frac{dn}{dz} = \frac{\partial n}{\partial z} + (v_g \cdot \nabla n) = \mathrm{St}n, \tag{5}$$

where $n(k, x)dkdx$ represents the power (number of particles) in a macroscopic volume element $dkdx$ of the phase space and Stn is a collision integral. Next, we consider the stationary regime $\partial n/\partial z = 0$ and assume that n depends on the position x via the temperature $T(x)$ and chemical potential $\mu(x)$. Further, we linearize Eq. (5), assuming small deviations from the local equilibrium, $n = n^{(0)} + \delta n$, where $n^{(0)}$ is the (local) equilibrium RJ distribution. Since $\mathrm{St}n^{(0)} = 0$, the rhs of Eq. (5) becomes $\mathrm{St}\delta n \approx -\delta n/z_T(k)$ ("time"-relaxation approximation). Then, the solution of the linearized KE reads

$$\delta n(k) \approx -z_T(k)\frac{n^{(0)}}{T}\left[(v_g \cdot \nabla\mu)n^{(0)} + (v_g \cdot \nabla T)\right], \tag{6}$$

resulting in power and heat currents

$$j_{a(q)} = \int \frac{dk}{(2\pi)} v_g(k)\left[\omega^{(J)}(k) - \mu\right]^s \delta n(k). \tag{7}$$

Evaluation of the above integrals (see Supplemental Material for details [21]) together with Eq. (2) leads to

$$\mathcal{L}_{aa} = -T^2\left[1 + \frac{\mu}{\sqrt{\mu^2 - 4J^2}}\right] z_T, \qquad \mathcal{L}_{qq} = 2J^2T^2 z_T,$$
$$\mathcal{L}_{aq} = \mathcal{L}_{qa} = -T^2\left[\mu + \sqrt{\mu^2 - 4J^2}\right] z_T, \tag{8}$$

where we omitted the k dependence of the relaxation distance z_T. Finally, within the linear response theory [$\nabla T \sim \Delta T/N \ll \bar{T} \equiv (T_L + T_R)/2$, $\nabla\mu \sim \Delta\mu/N \ll \bar{\mu} \equiv (\mu_L + \mu_R)/2$], we neglect the x dependence of temperature $T(x)$ and chemical potential $\mu(x)$ and approximate the Onsager elements as $\mathcal{L}_{ij}(T(x), \mu(x)) \approx \mathcal{L}_{ij}(\bar{T}, \bar{\mu})$. We find

that, contrary to the ballistic domain, $j_a, j_q \propto 1/N$ featuring the so-called normal transport, where the transport coefficients $\varkappa$, σ are independent of the system size and Fourier's law holds.

One-parameter scaling theory.—We have established a one-parameter scaling theory that controls the variation of j_a as the size of the junction increases. Specifically,

$$\frac{\partial p_N}{\partial lnN} = \beta(p_N), \qquad p_N(\chi, J, \bar{T}, \bar{\mu}) \equiv \frac{j_a}{j_a^{(\chi)}}, \tag{9}$$

where β is a function of the rescaled power current p_N alone. The renormalization of the current with its ballistic value $j_a^{(\chi)}$ scales out the details of the contact geometry (which is encoded in $j_a^{(\chi)}$), thus resulting in a contact-independent β function. Notice that $j_a^{(\chi)}$ can be exactly calculated using Eq. (3)—even for complex contacts where its numerical evaluation is always possible.

The scaling ansatz of Eq. (9) is equivalent to postulating the existence of a function $f(x)$ such that

$$p_N = f(\lambda \equiv N/l_T) \propto \begin{cases} 1; & \lambda \ll \mathcal{O}(1), \\ \frac{1}{N}; & \lambda \gg \mathcal{O}(1). \end{cases} \tag{10}$$

The scaling parameter $\lambda \equiv N/l_T$ encodes all the information about the relaxation process toward a nonequilibrium (quasi-)steady-state current and describes the number of thermalized segments with length $l_T \sim v_g z_T$ contained in a junction of length N. In the ballistic limit $l_T \gg N$, the junction consists of a single segment and the nonlinear interactions are unable to enforce thermalization of the modes. Therefore, the transport is essentially ballistic and $(j_a/j_a^{(\chi)}) \approx 1$. On the other hand, when $N \gg l_T$, the network consists of a number of $\lambda \gg 1$ uncorrelated segments. This situation is reminiscent of the law of additive resistances connected in series. As in this case, the total current decays inversely proportional to the number of segments $j_a \propto 1/N$. The relaxation distance that defines l_T is $z_T^{-1} \propto (\chi^2 a^2/J) \tanh\left[T/\zeta J a\right]$ and has been previously evaluated in Ref. [25] ($a \sim 1$ is the average value of norm per site, and $\zeta \approx 8$ is a best fitting parameter).

To validate our scaling ansatz (9), we have performed numerical simulations for various nonlinear coefficients χ, system sizes N, and temperatures T (see Fig. 2). Our simulations utilized two methods: (1) modeling the large collections of M modes in the bundles by Monte Carlo reservoirs [22] with effective thermostats at fixed (T, μ) (see filled symbols in Fig. 2); (2) solving numerically the TCMT (1) for the whole system reservoirs + junction) with reservoirs consisting of $M = 1600$ coupled modes forming a square lattice (see Supplemental Material [21]). The scaling ansatz (10) is also satisfied for negative temperature reservoirs (see orange asterisks in Fig. 2)—assuming that the linear response theory conditions are applicable. An

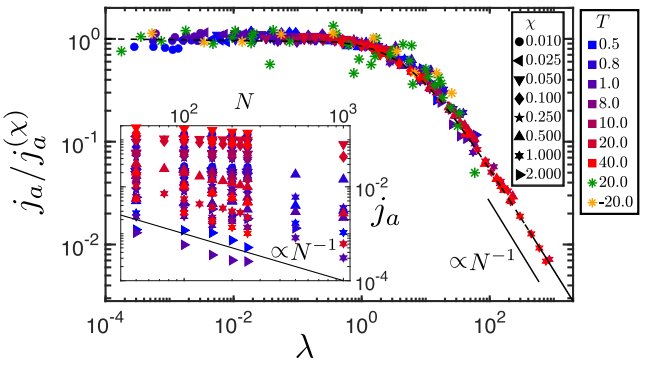

FIG. 2. Normalized power current $j_a/j_a^{(\chi)}$ versus the scaling parameter $\lambda = N/l_T$ for a 1D junction of (transverse) size N. The different values of the current j_a for a variety of parameters $(\chi, J, \bar{T}, \bar{\mu})$ are shown in the inset. The black dashed line is the interpolating function (11), while the solid line indicates a $1/N$ behavior and is drawn to guide the eye.

interpolating law that describes our data is

$$f(\lambda) = \frac{1}{1 + \lambda/\lambda_*}, \tag{11}$$

where $\lambda_* = 5.65$ is the best fitting parameter.

Photonic Wiedemann-Franz law and thermal current.—In thermoelectric devices, the Wiedemann-Franz (WF) law connects the thermal and current conductivity: their ratio is proportional to the temperature, i.e., $\varkappa/\sigma = LT$ with a constant L which, in typical metals, takes a universal value [32]. This proportionality relation indicates that a good electrical conductor is also an efficient heat conductor—a property that is rooted in the fact that heat and charge currents are associated with the flux of the same (quasi) particles. Deviations from the WF law signify the existence of multiple thermal and/or electrical flux transport mechanisms, enabling the independent control of electrical and thermal transport [31,33].

The equivalent of charge (particle) conductivity in photonics is power conductivity. It is natural, therefore, to extend the above definition of WF law and analyze the corresponding ratio of thermal conductivity to power conductivity. By combining Eqs. (4) and (8), we obtain

$$\frac{\varkappa}{\sigma} \approx \frac{J^2}{T}, \quad \text{for } |\mu| \gg (2J), \tag{12}$$

signifying a novel form of WF law that occurs in MMNPCs. This theoretical prediction is nicely confirmed by our simulations using Monte Carlo optical reservoirs (see main panel of Fig. 3). The various values of the nonlinear coefficient χ and junction size N that have been used in these simulations were chosen to guarantee that we have spanned the full transport domain from ballistic to diffusive regimes.

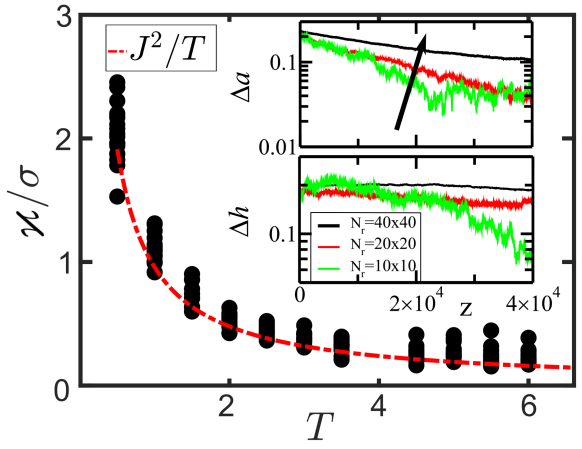

FIG. 3. The ratio of thermal to power conductivity $\varkappa/\sigma$ versus temperature (black dots) for different values of nonlinearities $\chi = 0$, 0.025, 0.05, 0.1, 0.25, 0.5, 0.75, 1.0, and junction sizes $N = 150$, 300, 600. The theoretical prediction (12) (red dashed line) indicates a $\propto 1/T$ behavior, signifying a separation of relaxation processes between thermal and power transport. In the insets, we show the difference of power (upper inset) and energy (lower inset) densities between the left and right reservoirs for three different reservoir sizes M. As M increases, the two reservoirs maintain for longer time their initial energy and power densities, allowing us to extract the (quasi)-steady-state values for the thermal and power currents.

The inverse temperature dependence of the ratio $\varkappa/\sigma$ signifies the decoupling of thermal and power transfer. A similar phenomenon has been also observed in ultracold atomic gases [34] implying that atom-atom interactions affect the associated thermal and particle conductivities in radically different ways. Specifically, it was shown that there is a timescale separation for the equilibration of temperature and particle imbalances between the two reservoirs. We have demonstrated the different equilibration times by performing dynamical simulations with small composite (junction + reservoirs) system sizes. In these simulations, we have utilized a microcanonical approach for the whole system and found different relaxation scales for the internal energy and power differences between the two reservoirs (see insets of Fig. 3).

Let us finally point out that, unlike the familiar case of metals, in the developed optical kinetics framework, the results for the WF law are sensitive to the definition of $\varkappa$. If, for example, we had defined the thermal conductivity under the constraint $\nabla\mu = 0$ (as opposed to the traditional $j_a = 0$ used above), we would end up with a different result for $\varkappa/\sigma$ [see Eqs. (S12) and (S19) of the Supplemental Material [21]]. In this case, at the high-temperature limit where $n^{(0)} \approx 1$, we get the familiar expression $\varkappa/\sigma \propto T$.

Conclusion.—We have developed an optical kinetics framework that predicts the response of MMNPCs in contact with optical reservoirs. Our methodology can be utilized for the design of all-optical cooling protocols and thermal rectifiers [35,36]. It will be interesting to extend our formalism to include transverse localization effects or the influence of paraxial noise (Markovian [37] or non-Markovian fluctuations where memory effects are important [38]) in the steady-state currents.

Note added.—Recently we became aware of Ref. [39] which analyzed the optical WF law using a microcanonical ensemble combined with the RJ power distribution. Their analysis is confined to the ballistic regime using Landauer's theory. Their results on the violation of the standard WF law are in agreement with ours.

We acknowledge partial support from the Simons Foundation for Collaboration in MPS Grant No. 733698. A. Y. R. and L. J. F.-A. acknowledge partial support from CONICET and MINCyT Grant No. CONVE-2023-10189190—FFFLASH and the hospitality of Wesleyan University. This work used computational resources from CCAD-UNC, which is part of SNCAD-MinCyT, and the high-performance computing cluster of IMIT (CONICET-UNNE), Argentina.

[1] G. Situ and J. W. Fleischer, Dynamics of the Berezinskii-Kosterlitz-Thouless transition in a photon fluid, Nat. Photonics **14**, 517 (2020).
[2] J. Klaers, J. Schmitt, F. Vewinger, and M. Weitz, Bose-Einstein condensation of photons in an optical microcavity, Nature (London) **468**, 545 (2010).
[3] C. Sun *et al.*, Observation of the kinetic condensation of classical waves, Nat. Phys. **8**, 470 (2012).
[4] A. Ramos, L. Fernandez-Alcazar, Tsampikos Kottos, and B. Shapiro, Optical phase transitions in photonic networks: A spin-system formulation, Phys. Rev. X **10**, 031024 (2020).
[5] K. Krupa, A. Tonello, B. Shalaby, M. Fabert, A. Barthélémy, G. Millot, S. Wabnitz, and V. Couderc, Spatial beam self-cleaning in multimode fibres, Nat. Photonics **11**, 237 (2017).
[6] Z. Liu, L. Wright, D. Christodoulides, and F. Wise, Kerr self-cleaning of femtosecond-pulsed beams in graded-index multimode fiber, Opt. Lett. **41**, 3675 (2016).
[7] A. Niang, T. Mansuryan, K. Krupa, A. Tonello, M. Fabert, P. Leproux, D. Modotto, O. N. Egorova, A. E. Levchenko, D. S. Lipatov, S. L. Semjonov, G. Millot, V. Couderc, and S. Wabnitz, Spatial beam self-cleaning and supercontinuum generation with Yb-doped multimode graded-index fiber taper based on accelerating self-imaging and dissipative landscape, Opt. Express **27**, 24018 (2019).
[8] L. G. Wright, D. N. Christodoulides, and F. W. Wise, Spatiotemporal mode-locking in multimode fiber lasers, Science **358**, 94 (2017).
[9] L. G. Wright, D. N. Christodoulides, and F. W. Wise, Controllable spatiotemporal nonlinear effects in multimode fibres, Nat. Photonics **9**, 306 (2015).
[10] K-P Ho and J. M. Kahn, *Mode Coupling and Its Impact on Spatially Multiplexed Systems*, Optical Fiber Telecommunications VIB (Elsevier, New York, 2013).

[11] D. Richardson, J. Fini, and L. Nelson, Space-division multiplexing in optical fibres, Nat. Photonics **7**, 354 (2013).
[12] F. O. Wu, A. U. Hassan, and D. N. Christodoulides, Thermodynamic theory of highly multimoded nonlinear optical systems, Nat. Photonics **13**, 776 (2019).
[13] K. G. Makris, F. O. Wu, P. S. Jung, and D. N. Christodoulides, Statistical mechanics of weakly nonlinear optical multimode gases, Opt. Lett. **45**, 1651 (2020).
[14] H. Pourbeyram, P. Sidorenko, F. O. Wu, N. Bender, L. Wright, D. N. Christodoulides, and F. Wise, Direct observations of thermalization to a Rayleigh-Jeans distribution in multimode optical fibres, Nat. Phys. **18**, 685 (2022).
[15] A. L. Marques-Muniz, F. O. Wu, P. S. Jung, M. Khajavikhan, D. N. Christodoulides, and U. Peschel, Observation of photon-photon thermodynamic processes under negative optical temperature conditions, Science **379**, 1019 (2023).
[16] K. Baudin, A. Fusaro, K. Krupa, J. Garnier, S. Rica, G. Millot, and A. Picozzi, Classical Rayleigh-Jeans condensation of light waves: Observation and thermodynamic characterization, Phys. Rev. Lett. **125**, 244101 (2020).
[17] K. Baudin, J. Garnier, A. Fusaro, N. Berti, C. Michel, K. Krupa, G. Millot, and A. Picozzi, Observation of light thermalization to negative-temperature Rayleigh-Jeans equilibrium states in multimode optical fibers, Phys. Rev. Lett. **130**, 063801 (2023).
[18] L. D. Landau and E. M. Lifshitz, *Physical Kinetics* (Pergamon Press, New York, 1981).
[19] M. Parto, F. O. Wu, P. S. Jung, K. Makris, and D. N. Christodoulides, Thermodynamic conditions governing the optical temperature and chemical potential in nonlinear highly multimoded photonic systems, Opt. Lett. **44**, 3936 (2019).
[20] C. Shi, T. Kottos, and B. Shapiro, Controlling optical beam thermalization via band-gap engineering, Phys. Rev. Res. **3**, 033219 (2021).
[21] See Supplemental Material at http://link.aps.org/supplemental/10.1103/PhysRevLett.132.193802 for additional information about the analytical calculations, numerical simulations, and possible experimental implementations, which includes Refs. [4,12,14,15,17,20,22–30].
[22] S. Iubini, S. Lepri, and A. Politi, Nonequilibrium discrete nonlinear Schrödinger equation, Phys. Rev. E **86**, 011108 (2012).
[23] H. B. Callen, *Thermodynamics and an Introduction to Thermostatistics* (John Wiley & Sons, New York, 1985).
[24] K. Saito, G. Benenti, and G. Casati, A microscopic mechanism for increasing thermoelectric efficiency, Chem. Phys. **375**, 508 (2010).
[25] A. Y. Ramos, C. Shi, L. J. Fernández-Alcázar, D. N. Christodoulides, and T. Kottos, Theory of localization-hindered thermalization in nonlinear multimode photonics, Commun. Phys. **6**, 189 (2023).
[26] Y. Imry and R. Landauer, Conductance viewed as transmission, Rev. Mod. Phys. **71**, S306 (1999).
[27] D. M. Basko, Kinetic theory of nonlinear diffusion in a weakly disordered nonlinear Schrödinger chain in the regime of homogeneous chaos, Phys. Rev. E **89**, 022921 (2014).
[28] E. Gerlach, J. Meichsner, and C. Skokos, On the symplectic integration of the discrete nonlinear Schrödinger equation with disorder, Eur. Phys J. **225**, 1103 (2016).
[29] P. J. Channell and F. R. Neri, An introduction to symplectic integrators, Field Inst. Commun. **10**, 45 (1996).
[30] C. J. Cattena, L. J. Fernández-Alcázar, R. Bustos-Marún, D. Nozaki, and H. M. Pastawski, Generalized multi-terminal decoherent transport: Recursive algorithms and applications to SASER and giant magnetoresistance, J. Phys. Condens. Matter **26**, 34 (2014).
[31] G. Benenti, S. Lepri, and R. Livi, Anomalous heat transport in classical many-body systems: Overview and perspectives, Front. Phys. **8**, 00292 (2020).
[32] N. W. Ashcroft and N. D. Mermin, *Solid State Physics* (Saunders College, Philadelphia, 1976).
[33] G. T. Craven and A. Nitzan, Wiedemann-Franz law for molecular hopping transport, Nano Lett. **20**, 989 (2020).
[34] M. Filippone, F. Hekking, and A. Minguzzi, Violation of the Wiedemann-Franz law for one-dimensional ultracold atomic gases, Phys. Rev. A **93**, 011602(R) (2016).
[35] L. J. Fernández-Alcázar, R. Kononchuk, H. Li, and T. Kottos, Extreme nonreciprocal near-field thermal radiation via Floquet photonics, Phys. Rev. Lett. **126**, 204101 (2021).
[36] S. Palafox, R. Román-Ancheyta, B. Çakmak, and Ö. Müstecaplıoğlu, Heat transport and rectification via quantum statistical and coherence asymmetries, Phys. Rev. E **106**, 054114 (2022).
[37] N. Berti, K. Baudin, A. Fusaro, G. Millot, A. Picozzi, and J. Garnier, Interplay of thermalization and strong disorder: Wave turbulence theory, numerical simulations, and experiments in multimode optical fibers, Phys. Rev. Lett. **129**, 063901 (2022).
[38] R. Román-Ancheyta, B. Çakmak, R. J. León-Montiel, and A. Perez-Leija, Quantum transport in non-Markovian dynamically disordered photonic lattices, Phys. Rev. A **103**, 033520 (2021).
[39] M. Lian, Y.-J. Chen, Y. Geng, Y. Chen, and J.-T. Lü, Violation of the Wiedemann-Franz law in coupled thermal and power transport of optical waveguide arrays, arXiv:2307.16529v1.